Original Paper

Cells Tissues Organs

Cells Tissues Organs 2003;174:117–128
DOI: 10.1159/000071152

Accepted after revision: February 12, 2003

Analysis of the Expression of Aquaporin-1 and Aquaporin-9 in Pig Liver Tissue: Comparison with Rat Liver Tissue

Neil C. Talbot[a] Wesley M. Garrett[a] Thomas J. Caperna[b]

[a]Gene Evaluation and Mapping Laboratory and
[b]Growth Biology Laboratory, Beltsville Agricultural Research Center, Beltsville, Md., USA

Key Words
Aquaporin · Antibody · Liver · Pig · Rat

Abstract
Aquaporins (AQPs) are cellular proteins involved with the movement of water across cell membranes and are fundamentally important to the fluid transport in the bile ducts and ductules of the liver. An immunohistochemical analysis of AQP-1 and AQP-9 was undertaken to describe their expression in fetal and adult pig liver, while immunoreagents specific to some other AQPs were screened for their efficacy on pig liver tissues. Anti-AQP-1 antibody reacted with the bile duct of the portal space and the bile ductules at the periphery of the liver lobules. Histological identification of bile ductules was confirmed by positive reactivity with anti-cytokeratin-7 and antilaminin immunostaining. Anti-AQP-1 signals were also pronounced in the endothelium of the portal space blood vessels and peripheral distributing venules. Antibody to AQP-9 reacted strongly with small ductules peripheral to the liver lobules, but only weakly with the bile ducts of the portal space. Anti-AQP-adipose antibody bound to the smooth muscle cells of the arteries in the portal space and sporadically with certain binucleated cells in the liver lobule. Antibodies to AQP-3, AQP-4, AQP-7, and AQP-8 were nonreactive with any of the tissues of the adult pig liver. For comparative purposes, immunohistochemical analysis of rat liver tissue was done with the anti-AQP-1 and AQP-9 antibodies. Anti-AQP-1 reacted weakly with the rat liver's bile ducts, but robustly with the endothelium of the liver's veins and arteries. It also reacted strongly with the central vein of the rat liver lobules, and, because the staining was continuous with hepatic sinusoids, it appeared that the reactivity was specific to the endothelial cells. Anti-AQP-9 antibodies reacted with rat hepatocytes and was not associated with the canaliculi,

Abbreviations used in this paper

Ab	antibody
AD	adipose
AQP	aquaporin
BME	β-mercaptoethanol
DIC	differential interference contrast
RBC	red blood cell
TBAG	20 m*M* Tris, 1 m*M* BME, 0.005% aprotinin, and 10% glycerol, pH 7.5
TBAK	20 m*M* Tris buffer containing 1% KCl, 0.005% aprotinin and 1 m*M* BME, pH 7.5

KARGER

Fax + 41 61 306 12 34
E-Mail karger@karger.ch
www.karger.com

1422–6405/03/1743–0117$19.50/0

Accessible online at:
www.karger.com/cto

Neil C. Talbot
US Department of Agriculture, Agricultural Research Service
Gene Evaluation and Mapping Laboratory, Bldg. 200, Rm. 13, BARC-East
Beltsville, MD 20705 (USA)
Tel. +1 301 504 8216, Fax +1 301 504 8414, E-Mail ntalbot@anri.barc.usda.gov

as judged by concurrent phalloidin staining of actin. The results indicate that specific AQPs are expressed in the tissues of the pig liver and that AQP-9 expression is distinct from its expression in the rat liver.

Introduction

Aquaporins (AQPs) are a group of sequence-related proteins involved with the movement of water across cell membranes that are highly conserved across species [Schulte and Van Hoek, 1997; Ma and Verkman, 1999; Engel et al., 2000]. The AQPs (AQP-0 to AQP-9) span cell membranes to form channels that are either selective for the transport of water (AQP-1, AQP-2, and AQP-4 to AQP-6) or water and polar solutes (AQP-3 and AQP-7 to AQP-9) such as glycerol and urea [Ma and Verkman, 1999]. Individual monomeric units of the AQPs are proteins of ~30 kD. They occur in nonglycosylated or glycosylated forms that associate as homotetramers with each monomer possessing an independent water channel [Shi et al., 1994; Schulte and Van Hoek, 1997]. Arrays of AQP tetramers apparently mediate the rapid flow of water within a variety of tissues or cells where fluid transport and homeostasis are important [Ma and Verkman, 1999; Engel et al., 2000].

AQPs have been shown to be expressed in the liver and biliary epithelium [Marinelli and LaRusso, 1997; Ma and Verkman, 1999; Schrier et al., 2001]. AQP-1 protein expression was detected by various methods, including immunocytochemistry, in the bile duct cells of rats and humans [Nielsen et al., 1993; Roberts et al., 1994]. Conversely, AQP-1 protein was not found in the hepatocytes of the liver [Nielsen et al., 1993; Roberts et al., 1994]. AQP-1 was also expressed in human liver capillary endothelium and the endothelial cells of other organs [Nielsen et al., 1993]. Other AQPs reportedly expressed in liver tissue include AQP-8 and AQP-9. AQP-9 expression was located in the plasma membrane of hepatocytes in the rat liver as determined by immunocytochemistry and immunoelectron microscopy [Elkjær et al., 2000]. AQP-8 was specifically located in the cytoplasm and cytoplasmic membranes of hepatocytes [Garcia et al., 2001]. Other AQP family members have not yet been reported in liver tissue.

Our laboratory is involved with developing in vitro models of embryonic and adult pig liver and biliary epithelium [Talbot et al., 1996; Talbot and Caperna, 1998]. The functional validity of these in vitro models is in part dependent on knowledge of normal pig hepatocyte and bile duct epithelium protein expression [Talbot et al., 2003]. Since cross-species differences in the expression of AQPs are becoming apparent [King and Agre, 2001], an immunocytochemical study was undertaken to describe the developmental expression of AQPs in the normal pig liver. The results show that AQP-1, AQP-adipose, and AQP-9 are expressed in pig liver and that the specific cell expression of AQP-9 is different from that found in the rat liver.

Materials and Methods

Fluorescent Phalloidin Labeling and Antibody Analysis

Pig liver tissue samples were freshly isolated from 40- and 90-day fetal pigs and adult pigs. In addition to liver tissue, kidney and lung tissue samples were also taken from the pigs. The tissue samples were immersed in Tissue-Tek OCT compound (Miles, Elkhart, Ind., USA) in Peel-A-Way disposable embedding molds (Polysciences, Warrington, Pa., USA) and frozen in a dry ice ethanol bath. Frozen sections were cut at a thickness of 5 μm on a Hacker-Bright cryostat (Hacker Instruments, Fairfield, N.J., USA) and thaw-mounted onto Superfrost Plus microscope slides (Fisher Scientific, Pittsburgh, Pa., USA). Samples of adult rat liver tissue were similarly processed.

The procedure used for immunostaining frozen sections was essentially identical to the one described previously [Garrett and Guthrie, 1996] except that in the present study tissue sections were fixed briefly in 10% neutral buffered formalin, and primary antibodies were detected by immunofluorescence. Rabbit polyclonal antibodies to rat AQP-1, AQP-3, AQP-4, AQP-7, AQP-8, AQP-9 and human AQP-adipose (AQP-AP, AQP-7L or AQP-7) were purchased from Alpha Diagnostic International (San Antonio, Tex., USA) and used at a concentration of 5 μg/ml. Mouse monoclonal antilaminin (clone LAM-89; Sigma Chemical Co., St. Louis, Mo., USA) was used at a dilution of 1:2,000, and mouse monoclonal anti-cytokeratin-7 (clone OVTL 12–30; Cappel, Organon Teknika, Durham, N.C., USA) was used at a concentration of 5 μg/ml. Rabbit and mouse primary antibodies were detected with either Alexa Fluor 488 goat anti-rabbit IgG or Alexa Fluor 594 goat anti-mouse IgG (Molecular Probes, Eugene, Oreg., USA) at dilutions of 1:400. In some cases the actin cytoskeleton was stained with Alexa Fluor 594 phalloidin (Molecular Probes) at 2 units/ml (66 n*M*). Cell nuclei were counterstained with 2 μg/ml bisbenzimide (Hoechst 33342; Molecular Probes) and the specimens were mounted in Vectashield (Vector Labs, Burlingame, Calif., USA).

Images were acquired in frame mode with a Zeiss LSM 410 (Carl Zeiss, Thornwood, N.Y., USA) confocal microscope through a 63× C-Apochromat 1.2 NA water immersion objective. The 351-nm line of a Coherent Innova 90 (Coherent, Santa Clara, Calif., USA) laser was used to excite H 33342, and emitted light was passed through a long-pass 397-nm filter. The 488- and 568-nm lines of an Omnichrome (Omnichrome, Chino, Calif., USA) Ar/Kr laser were used to excite Alexa Fluor 488 and 594, respectively. A bandpass 515- to 540-nm filter was used for the green-emitting Alexa Fluor 488, and a long-pass 590-nm filter for the red-emitting Alexa fluor 594. Individual optical sections were digitally recombined into a single composite

image using LSM software (Carl Zeiss). Bright-field differential interference contrast images were captured with the transmitted light detector using the 633-nm line of the internal He/Ne laser for illumination.

Additional images were acquired with a Zeiss Axioskop (Carl Zeiss) fitted with a Spot (Diagnostic Instruments, Sterling Heights, Mich., USA) digital camera. Fluorochromes were viewed with the following filter sets: a G 365-nm excitation filter, FT 395-nm dichroic beamsplitter and LP 420-nm emission filter for H 33342, BP 450- to 490-nm excitation filter, FT 510 dichroic beamsplitter and LP 515 emission filter for Alexa Fluor 488, and BP 510- to 560-nm excitation filter, FT 580-nm dichroic beamsplitter, and LP 590-nm emission filter for Alexa Fluor 594.

Western Immunoblot Analysis

Interlobule bile duct tissue, whole liver tissue, and red blood cells (RBC) were collected from a normal adult pig. Normal adult rat liver and bile duct tissue was similarly collected by dissection of the liver. Tissues were minced in 20 m*M* Tris buffer containing 1% KCl, 0.005% aprotinin and 1 m*M* β-mercaptoethanol (BME), pH 7.5 (TBAK), homogenized mechanically (Omni 2000, Omni Int., Waterbury, Conn., USA), briefly sonicated with a microprobe (Model XL, Misonix, Farmingdale, N.Y., USA) and centrifuged at 105,000 *g* for 30 min at 4°C. Supernatants were aspirated and membranes were resuspended in buffer containing 20 m*M* Tris, 1 m*M* BME, 0.005% aprotinin, and 10% glycerol, pH 7.5 (TBAG) by sonication. Red cell membranes were obtained by repeatedly washing whole blood cells (collected in the presence of EDTA) in normal saline to remove plasma and leukocytes and by final sonication in TBAK buffer. Tissue lysates and membrane material were sonicated prior to analysis of protein concentration by a modified Lowry procedure [Nerurkar et al., 1981], using bovine serum albumin as standard.

Tissue lysates and membrane fractions were separated by SDS-PAGE (Mini Protean-3, BioRad, Hercules, Calif., USA) and were blotted onto 0.2-μm pore nitrocellulose using a semidry blotting system (BioRad). All samples were boiled (5 min) in gel loading buffer containing 62.5 m*M* Tris, 1 m*M* EDTA, 5% BME, 6% glycerol and 1.5% SDS, pH 7.0. In preparation for each immunoblot, specific amounts of protein were loaded (anti-AQP-1 immunoblot = 24 μg for liver tissues and 6 μg for RBC membranes; anti-AQP-9 immunoblot = 30 μg; anti-cytokeratin-7 = 18 μg) in 40 μl for each lane of 1.5 mm thick, 12% acrylamide gels. Following electrophoresis and electrotransfer onto nitrocellulose, blots were stained with fast green to visualize total proteins. Blots for cytokeratin-7 were blocked for nonspecific reactions by overnight incubation in Tris-saline containing 3% bovine serum albumin (Sigma, A7888) and 3% nonfat dry milk (Carnation, Nestlé Food, Glendale, Calif., USA) and, for AQP-1 and AQP-9, in 5% nonfat dry milk. After washing, blots were incubated with mouse anti-cytokeratin-7 (1/750, clone OVTL 12–30 Cappel Research Products, Durham, N.C., USA) or affinity-purified rabbit anti-AQP-1 or anti-AQP-9 (1/1,200 and 1/1,250, respectively, Alpha Diagnostics) in Tris-saline containing blocking protein and 0.1% Tween 20. For competitive inhibition assays of AQP-1 and AQP-9, their respective antigenic peptides were purchased from Alpha Diagnostics and they were used at a 50-μg peptide to 6-μg antibody (8:1) ratio in the immunoblot's primary reaction. Alkaline phosphatase-conjugated (A2256 and A2179; Sigma) or horse radish peroxidase-conjugated (NA9340; Amersham Biosciences, Little Chalfont, UK) secondary antispecies antibodies were applied in the same buffer for 1.5 h. The presence of specific proteins was evaluated by a colorimetric alkaline phosphatase detection system (BCIP/NBT, Sigma) or ECLplus (Amersham). Stained nitrocellulose blots or X-ray films were scanned with a digital imaging system (Chemimager 4000, Alpha Innotech, San Leandro, Calif., USA).

Results

AQP Expression in 40- and 90-Day Fetal Pig Liver

The histological presentation of the 40- and 90-day fetal pig liver tissue was similar, and, in general, the tissue was composed of areas of hepatoblasts extensively interspersed with areas of hematopoietic cell development, or blood islands, as is normally found in the developing liver [Enzan et al., 1997; Timens and Kamps, 1997]. Overall the tissue structure was unorganized compared to the adult pig liver with no lobular structure or bile duct network evident. However, more areas of cuboidal cells forming duct-like structures were found at the later gestational time point. Positive laminin signals were associated with these duct-like structures, and anti-cytokeratin-7 antibody binding was also detected in the cells if a morphologically definable ductal structure existed (fig. 1A, B). Therefore, these cells were presumably areas of nascent bile duct development. Anti-AQP-1 reacted strongly with the cells in the blood islands of the 40-day and 90-day pig liver, and positive reactivity with the ductular structures was also observed (fig. 1A–D). Anti-AQP-9 antibody immunostaining was negative for the 40-day liver tissue except for a strong reaction with the surface of the fetal liver (fig. 1E). In 90-day liver tissue, the anti-AQP-9 reacted positively with the developing ductal structures (fig. 1F). Immunolabeling with anti-AQP-AD was not found, and, in addition, antibodies to AQP-3, AQP-4, AQP-7 and AQP-8 did not react positively with any cells of the pig fetal liver (data not shown).

AQP Expression in Adult Pig Liver

The adult pig liver tissue was composed of well-defined classic lobules containing a central vein. Portal spaces occurring between adjacent lobules were observed to contain bile ducts that were labeled positively with anti-cytokeratin-7 and antilaminin antibodies (fig. 2A, B). The portal spaces also contained interlobular branches of the portal vein, muscular arteries branching out from the hepatic artery, and lymphatic vessels. Smaller distributing veins, emanating from the portal vein, and smaller bile ductules were observed around the periphery of the lobules. These peripheral bile ductules were also positive for reaction with anti-cytokeratin-7 and antilaminin antibodies (not shown). Anti-AQP-1 immunolabeling oc-

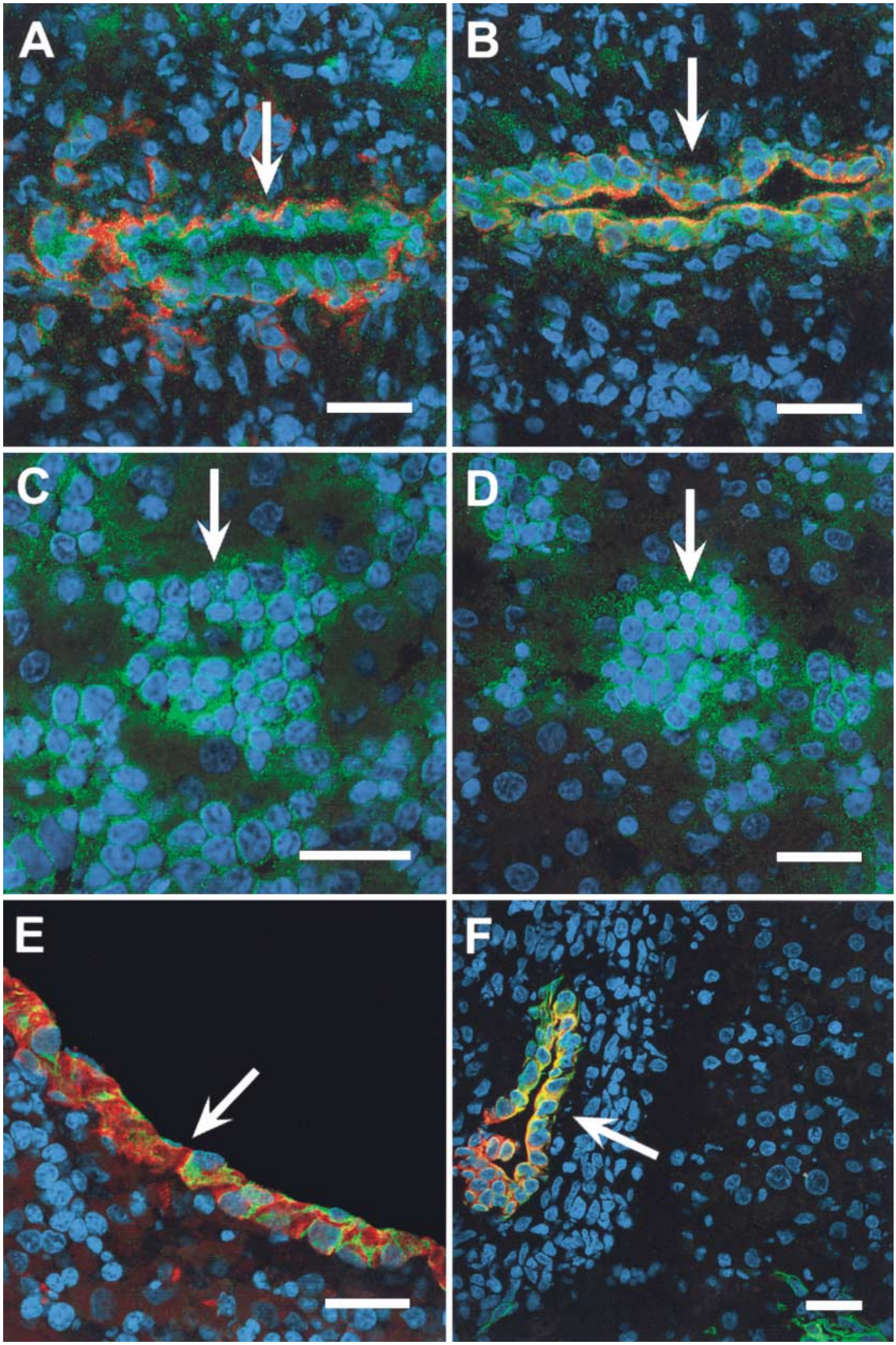
A
B
C
D
E
F

curred in the bile duct cells in both the major bile ducts of the portal space and also, though not as strongly, in the peripheral bile ductules in between the lobules (fig. 2C, D). Endothelial cells lining the portal space blood vessels were also positive for anti-AQP-1 reactivity, as were the cells of the smaller venules in between lobules (fig. 2B). Hepatocytes and sinusoids were negative for anti-AQP-1 staining as were the central veins of the lobules (fig. 2D). In contrast to AQP-1, the biliary epithelium of the portal space bile ducts was faintly stained by anti-AQP-9 antibody whereas the cholangiocytes of the bile ductules running between or within the lobules were robustly stained (fig. 3). Endothelial cells of arteries were negative for anti-AQP-9 reactivity (fig. 3). Positive signals from reaction with the anti-AQP-AD were found in the smooth muscle cells of the arteries and veins of the portal spaces (fig. 4A, B). Also, anti-AQP-AD antibody gave sporadic, but distinctly localized staining, within the pig liver lobule. Two relatively small, closely associated, nuclei were present in the centers of each of the anti-AQP-AD-stained areas in the liver lobule (fig. 4C, D). Presumably this indicated a binuleated cell. As with fetal tissues, the antibodies to AQP-3, AQP-4, AQP-7, and AQP-8 did not react positively with any of the tissues of the adult pig liver (data not shown).

AQP Expression in the Adult Rat Liver

As a comparative control, the antibodies to AQP-1 and AQP-9 were tested on cryostat sections of adult rat liver tissue. Anti-AQP-1 binding was pronounced on the surface of the rat liver's central vein, presumably reacting with the endothelial cells lining the central vein (fig. 5A). The anti-AQP-1 antibody reacted weakly with rat bile ductules of the portal triad (fig. 5C). The characteristic histological presentation of the portal triad was highlighted by fluorescent staining of actin with phalloidin. More pronounced anti-AQP-1 antibody reactivity was found in the endothelium of veins and arteries than in the bile ducts (fig. 5C). Strong, but sporadic, anti-AQP-1 signals were also present amongst the hepatocytes of the rat liver (fig. 5A, E). Fluorescent phalloidin staining of the actin cytoskeleton, which highlighted the canaliculi between hepatocytes, indicated that the anti-AQP-1 staining was not coincident with the canaliculi (fig. 5E). Therefore, while the AQP-1 reactivity appeared to be within the sinusoids, it was unclear whether the hepatocytes or endothelial cells lining the sinusoids were labeled. Anti-AQP-9 reactivity was strong and extensive across the rat liver lobule, and it appeared to label the sinusoids between hepatocytes as, like AQP-1 staining, it was not coincident with the canaliculi revealed by phalloidin staining (fig. 5B, F). However, it was unclear whether the endothelial cells lining the sinusoids or the cytoplasmic membranes of the hepatocytes were labeled by the anti-AQP-9 antibody. In stark contrast to the staining by the anti-AQP-1 antibody, the anti-AQP-9 antibody did not react with bile duct cells or the endothelium of the veins and arteries in the rat liver (fig. 5D).

Immunoblot Analysis of Rat and Pig Liver Tissue

To test the specificity of the AQP antibodies and the character of the protein bound by the antibodies, Western blots of pig and rat liver tissues were probed with the antibodies. RBC membranes were also analyzed as a positive control for AQP-1 expression. As shown in figure 6A, anti-AQP-1 antibody reacted with multiple protein bands spanning approximately 33–43 kD, and a single lower molecular weight band of approximately 26 kD in both pig and rat RBC membranes. This pattern of reactivity has been previously reported for purified AQP-1, or CHIP28 protein, where the higher molecular weight diffuse bands are the glycosylated forms of the protein and the sharper lower molecular weight band is the nonglycosylated form [Agre et al., 1993]. The same lower molecular weight protein was also detected by the anti-AQP-1 in pig bile duct membranes, rat bile duct whole tissue extract, and rat liver membrane (fig. 6A). The anti-AQP-1 antibody also reacted with a protein of ~30 kD in the rat bile duct whole tissue extract (fig. 6A). Pig liver membrane preparations were negative for reactivity with the anti-AQP-1 antibody indicating that the protein was either not present or was too small a proportion of the liver tissue sample to be detectable (fig. 6A, lane 2). This would be consistent with the immunocytochemical presentation

Fig. 1. Triple- or double-staining immunohistochemical analysis of 40- or 90-day fetal pig liver frozen sections with antibody (Ab) to AQP-1 and AQP-9. **A** Ninety-day ductal structure (arrow); antilaminin Ab (red), anti-AQP-1 Ab (green), and Hoechst-labeled nuclei (blue). Note basal lamina staining of the ductal cells with the antilaminin Ab and positive cytoplasmic staining with AQP-1 Ab. **B** As in **A** except red signal is anti-cytokeratin-7 Ab reaction. **C** Forty-day fetal liver; note positive reaction of anti-AQP-1 Ab (green) within the cytoplasm of hemopoietic cells in blood islands (arrow). **D** As in **C** in the 90-day liver. Anti-AQP-9 Ab (green) labeling of external surface of day-40 fetal pig liver (arrow); red is antilaminin signal (**E**), and of ductal structures (arrow) at 90 days; anti-cytokeratin-7 labeling is red signal (**F**). Scale bar ≈ 25 μm.

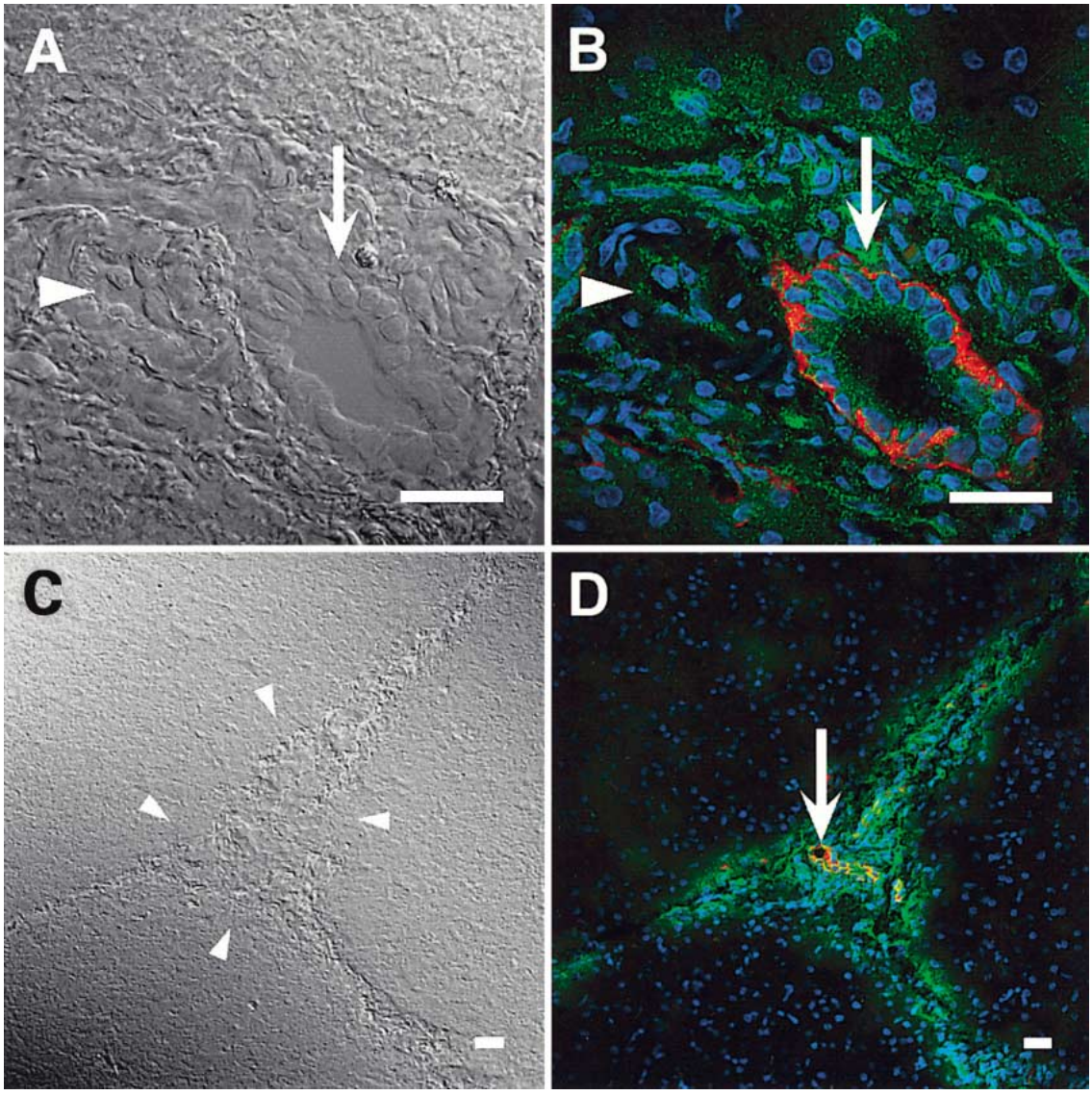

2

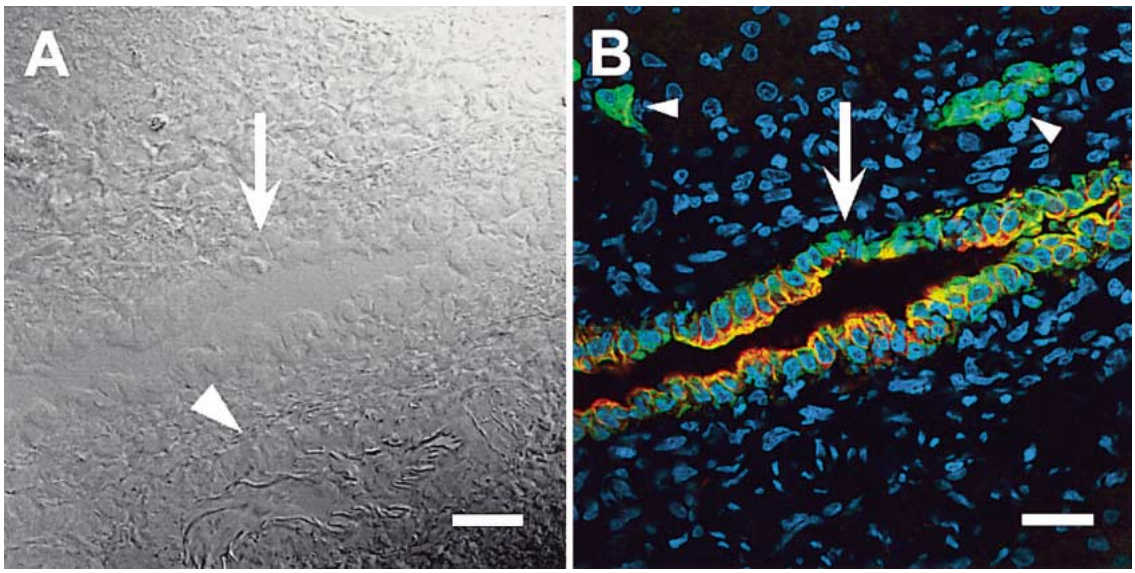

3

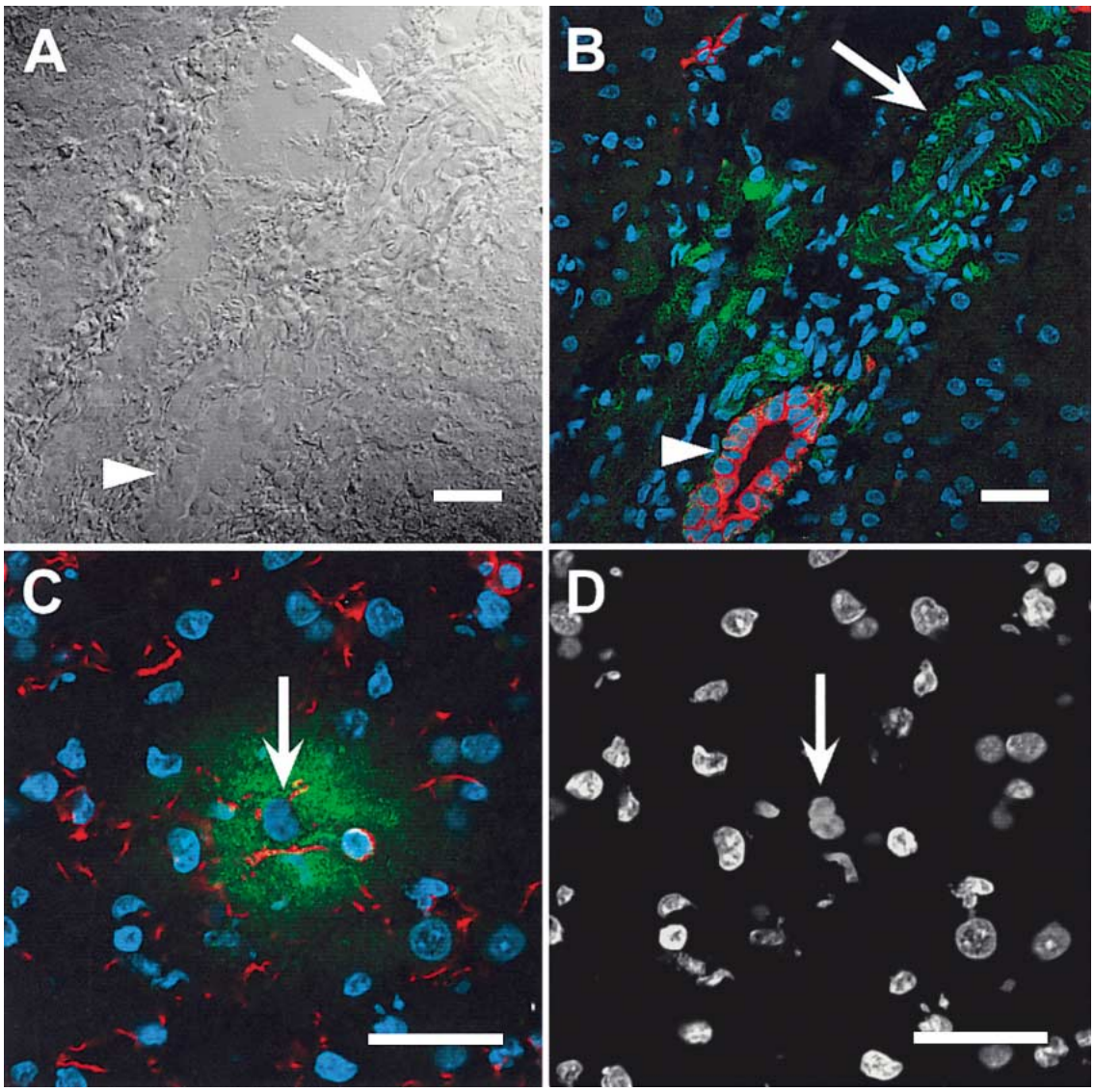

4

Fig. 2. Triple-staining immunohistochemical analysis of adult pig liver frozen sections with anti-AQP-1 antibody (Ab). **A** Differential interference contrast (DIC) image showing bile duct (arrow) and associated artery (arrowhead). **B** Same area as in **A** showing basal antilaminin Ab staining (red) of the bile duct and anti-AQP-1 reactivity (green) of the bile duct cells, the artery, and associated venous tissue; Hoechst-labeled nuclei are blue. **C** Lower power DIC image showing portal triad area (arrowheads) between three liver lobules. **D** Same area as in **C** showing anti-AQP-1 Ab reactivity (green) with bile duct (arrow) and associated blood vessels; note bile duct is also positively labeled from reaction with anti-cytokeratin-7 Ab (red). Scale bar ≈ 25 μm.

Fig. 3. Triple-staining immunohistochemical analysis of adult pig liver frozen sections with anti-AQP-9 antibody (Ab). **A** Differential interference contrast image of bile duct (arrow) and artery (arrowhead). **B** Same area as in **A** showing positive anti-AQP-9 Ab reaction (green) with bile duct and distributing bile ductules (arrowheads) and positive anti-cytokeratin-7 Ab reactivity (red) with the same; Hoechst-stained nuclei are blue. Note nonreaction of Abs with arterial tissue. Scale bar ≈ 25 μm.

Fig. 4. Triple-staining immunohistochemical analysis of adult pig liver frozen sections with anti-AQP-AD antibody (Ab). **A** Differential contrast image of bile duct (arrowhead) and artery (arrow; cut tangentially). **B** Same area as in **A** showing labeling of arteries with anti-AQP-AD Ab (green) and no reaction with bile duct; red signal is anti-cytokeratin-7 Ab reaction and nuclei are labeled blue (Hoechst). **C** High-power triple-stained image of cells within the liver lobule showing an area (arrow) of positive anti-AQP-AD reactivity (green) and positive labeling of associated nonparenchymal cells with antivimentin Ab (red). **D** Same area as in **C** showing Hoechst-labeled nuclei only; note typical, apparently binucleated, cell that is coincident with the anti-AQP-AD Ab reactivity (arrow). Scale bar ≈ 25 μm.

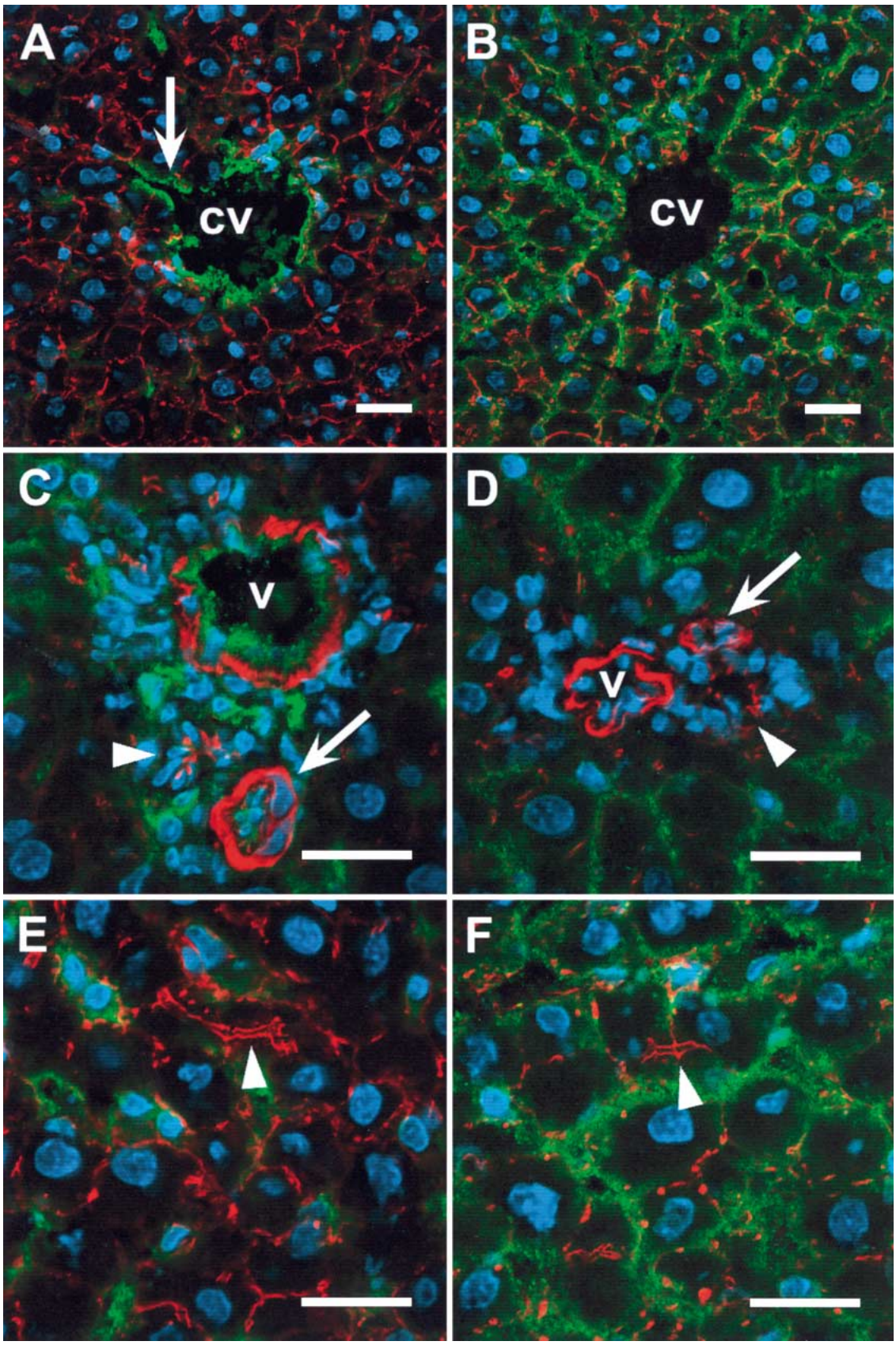

5

since peripheral bile ductules between lobules were weakly stained by the antibody and bile ductules within the lobules, hepatocytes and sinusoids were not stained at all by the antibody. All of the protein bands reactive with the anti-AQP-1 antibody were eliminated by the addition of AQP-1 peptide antigen to the immunoblot reaction and the reaction of the Western blots with secondary antibody alone also produce no signal (data not shown).

Anti-AQP-9 antibody was positive for reaction with pig bile duct membranes, a single protein band of approximately 42 kD, and with pig whole liver membranes, a single protein band of approximately 33 kD (fig. 6B). Reaction with the pig whole liver membrane preparation is consistent with the immunocytochemical results in that the bile ductules running between and within the pig liver lobules were highly stained by the anti-AQP-9 antibody. At least two protein bands were detected in the rat bile duct and liver protein preparations by the anti-AQP-9 antibody. Their apparent molecular weights were approximately 29–33 kD. All of the protein bands reactive with the anti-AQP-9 antibody were eliminated by the addition of AQP-9 peptide antigen (data not shown).

Antibody to cytokeratin-7 was also tested against the panel of pig and rat tissues. A group of proteins spanning 41–48 kD was reactive in the pig bile duct tissue (fig. 6C, lane 1). Pig whole liver, rat bile duct, and rat whole liver tissue membranes were nonreactive with the anti-cytokeratin-7 antibody.

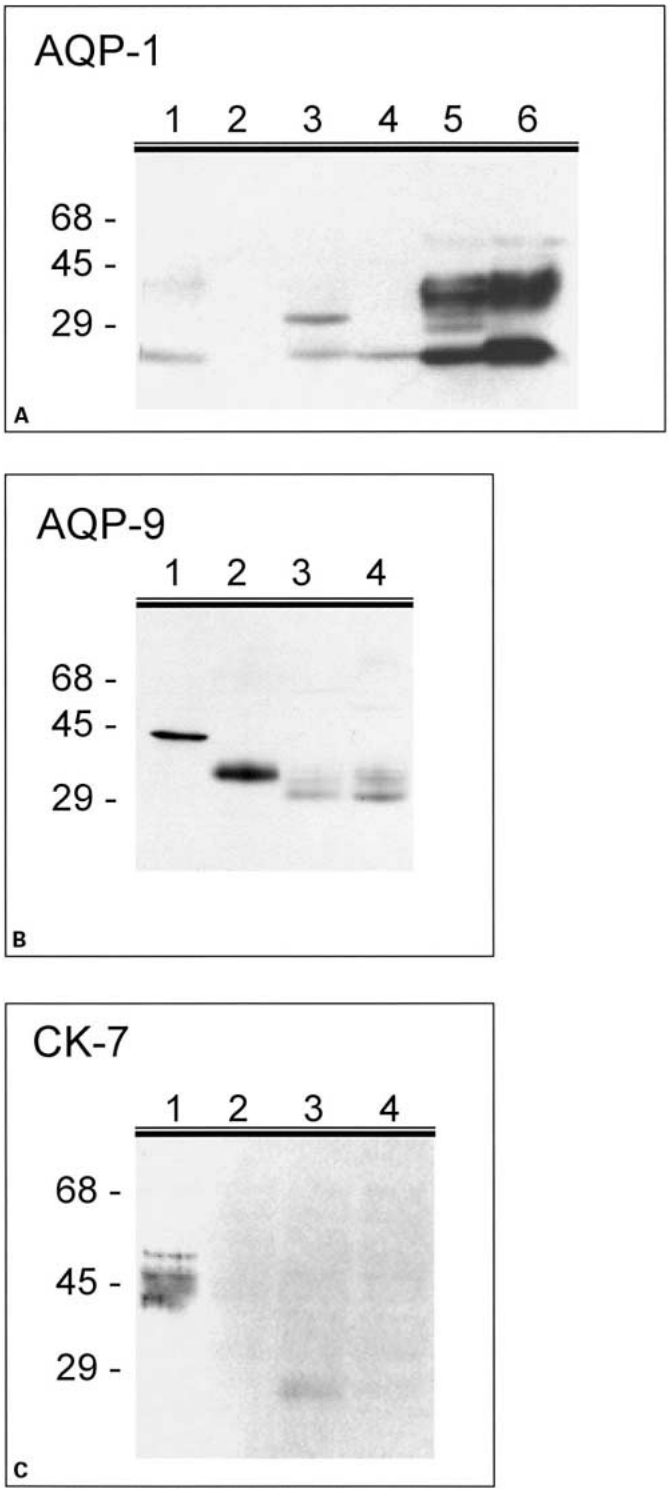

Fig. 6. Western immunoblot analysis of pig and rat liver tissues with antibodies to AQP-1 (**A**), AQP-9 (**B**) or cytokeratin-7 (**C**). Protein preparations were as follows: lane 1 = pig bile duct membrane; lane 2 = pig whole liver membrane; lane 3 = rat whole bile duct membrane; lane 4 = rat whole liver membrane; lane 5 = pig RBC membrane; lane 6 = rat RBC membrane.

Fig. 5. Triple-stained immunohistochemical analysis of adult rat liver frozen sections with anti-AQP-1 or anti-AQP-9 antibody (Ab). **A** Central vein (CV) area of a rat liver lobule showing anti-AQP-1 labeling (green) of the surface of the CV and connecting sinusoid (arrow); phalloidin-labeled actin cytoskeletal elements are red and Hoechst-labeled nuclei are blue. **B** CV area of rat liver lobule showing uniform anti-AQP-9 Ab labeling throughout the sinusoids (green); actin (red) as in **A**. **C** Portal triad area showing positive anti-AQP-1 reactivity (green) with vein (V), artery (arrow), and bile duct (arrowhead); red signal is actin staining. **D** Portal triad area showing negative reactivity of anti-AQP-9 Ab with vein (V), artery (arrow), and bile duct (arrowhead); red signal is actin staining. **E** Higher magnification of anti-AQP-1 Ab reaction (green) within liver lobule; note the sporadic labeling of hepatocytes and sinusoids and that the labeling is not associated with canaliculi (arrowhead), which are delineated by the phalloidin labeling of the actin cytoskeleton (red). **F** Higher magnification of anti-AQP-9 Ab reaction (green) within liver lobule; note extensive labeling of the sinusoidal surfaces and that the labeling is not associated with canaliculi (red actin signal; arrowhead). Scale bar ≈25 μm.

Anti-AQP-8 antibody gave a dominant band (or two bands for rat tissue) of ~38 kD in size. This dominant anti-AQP-8 signal was strongest in both pig and rat whole liver tissue, but was also present in bile duct tissue, and several additional, apparently spurious protein bands were also reactive with the antibody (data not shown). Anti-AQP-4 and anti-AQP-AD were also tested, but against a Western blot of pig liver or bile duct samples only, and the results were either negative or unclear, respectively (data not shown).

Discussion

The results indicate that AQP-1 and AQP-9 proteins are expressed in fetal and adult pig liver. In the fetal pig liver AQP-1 expression was most pronounced in the cells of the liver's blood islands and this was easily detected at 40-day gestation. This is in accord with other reports where AQP-1 has been found in the RBCs of various species [Agre et al.,1993; Schulte and van Hoek, 1997; Talbot et al., 2003]. AQP-1 expression in the pig liver bile duct was first detectable in the 90-day fetal liver and was always coincident with positive cytokeratin-7 and laminin immunostaining, indicating formations of nascent bile ducts. This early expression in the bile duct epithelium continues in the adult pig bile ducts and ductules and is similar to previous findings in rat liver [Nielsen et al., 1993; Roberts et al., 1994; Marinelli et al., 1999]. The results also showed that AQP-1 is highly expressed in the endothelial cells lining the blood vessels of the pig liver. The relatively high expression in the blood vessel endothelium was also found in rat liver by Marinelli et al. [1999], who used the same anti-AQP-1 antibody employed here. Our own comparative analysis of rat liver tissue was in agreement with results reported by Marinelli et al. [1999], showing weak expression in the bile ducts and intense expression in the blood vessels. However, the present results indicate that AQP-1 is also expressed on the endothelial cells lining the central vein of the rat liver and that this expression continues, although sporadically, across the liver lobule. Coincident staining with fluorescently labeled phalloidin, which highlights canalicular connections by virtue of specific interaction with F-actin, indicated that the AQP-1 expression across the rat liver lobule was located at the hepatic sinusoids (fig. 5). Therefore, taken together with the continuous connection of the AQP-1 signal with the surface of the central vein, it seems likely that the AQP-1 expression is in the endothelial cells of the rat liver lobules. This interpretation is consistent with previous published data that indicate no AQP-1 expression in purified rat hepatocytes [Roberts et al., 1994].

AQP-9 expression in the pig liver appeared to be limited to the bile duct tissue, and, particularly, to the smaller distributing bile ductules running between and within the liver lobules. This is in contrast to the expression pattern reported by other laboratories for rat liver tissue where AQP-9 was immunolocalized to the hepatocytes and especially along the sinusoidal surface or facing the space of Disse [Elkjær et al., 2000; Nihei et al., 2001; Huebert et al., 2002]. These studies used the same commercial anti-AQP-9 antibody, and our results of the analysis of AQP-9 expression in the rat liver are in agreement with these previous findings (fig. 5). Thus, AQP-9 expression in the pig is distinct from its expression in the rat liver.

The immunoblot for AQP-9 produced one distinct band of approximately 42 kD in the pig bile duct tissue (fig. 6B, lane 1) and one smaller distinct band of approximately 33 kD in the pig whole liver membranes (fig. 6B, lane 2). This result indicates that in the pig differential forms of the AQP-9 protein are expressed in the bile duct tissue depending on whether it is extrahepatic or intrahepatic. Evidence for higher molecular weight forms in rat liver tissue was recently reported by Nicchia et al. [2001] using the same anti-AQP-9 antibody. They found 32- to 34-kD forms of AQP-9 as the major reactive bands in their analysis and also found that, in contrast to AQP-1, the higher molecular weight AQP-9 forms were not glycosylated [Nicchia et al., 2001]. It is interesting to note that a higher molecular weight form was found in the pig bile duct, and that it appears to be a distinctly larger form of AQP-9 compared to that expressed in the pig interlobule and intralobule bile ductules. A similar higher molecular weight (42 kD) anti-AQP-9 protein band was also found in immunoblots of pig gall bladder tissue [Talbot and Caperna, unpubl. data]. We are currently analyzing these alternative forms of anti-AQP-9-reactive proteins by 2-dimensional gel electrophoresis and mass spectroscopy.

Antibodies to human AQP-AD, which apparently shares identity with AQP-7 [Ishibashi et al., 1998], displayed two separate reactivities within the pig liver. The first was with the smooth muscle cells of the arteries and veins of the portal space. Other AQPs have been found in muscle. For example, AQP-4 was reported to be expressed in the sarcolemma of the skeletal muscle fibers [Frigeri et al., 1998] and AQP-1 in the smooth muscle fibers of rat female reproductive tract, cardiac myocytes and vascular smooth muscle cells of large arteries [Gannon et al., 2000]. The second reactivity of the anti-AQP-AD was

with occasional cells that were intimately associated with hepatocytes within the liver lobule. The nuclei of the cells were characteristically smaller than the surrounding hepatocyte nuclei and occurred in pairs giving the impression that the anti-AQP-AD-positive cells were binucleated (fig. 4C, D). Since AQP-7 is expressed in adipocyte, double staining with antivimentin antibody to identify Ito cells (fat-storing cells) was performed. The vimentin-positive cells, perhaps macrophages as well as Ito cells, did not have a unique association with the anti-AQP-AD signal, although they were coincident, and, therefore, the identity of the cells reactive with the anti-AQP-AD antibody remains undefined.

The antibodies used in this study were all generated from rat-specific peptide sequences (Alpha Diagnostics). While specific cross-reactivity with pig liver tissue was evident for anti-AQP-1 and anti-AQP-9 from the immunohistochemical and immunoblot results, cross-species reactivity of the other anti-AQPs was inconsistent or not found. For example, the anti-AQP-8 antibody reacted similarly with both rat and pig liver tissue by immunoblot assay, but was not found to be reactive by immunohistochemical assay (data not shown). This is in contrast to the recently published results in rat liver using the same antibody [Garcia et al., 2001; Tani et al., 2001; Huebert et al., 2002]. Tani et al. [2001] demonstrated the antibody's specificity by immunoblot and further showed that the immunohistochemical reactivity was located in the canaliculi between the rat hepatocytes. It appears, therefore, that the antibody does not cross-react with pig liver tissue by the immunohistochemical technique used here, i.e. cryosections treated briefly with 10% neutral buffered formalin.

Information about AQP expression in the pig liver will provide a basis with which to assess the functional validity of in vitro models of pig hepatocytes and pig bile duct cells [Talbot et al., 1996; Talbot and Caperna, 1998]. Recently, we have found that pig bile ductules, grown and differentiated in vitro, rapidly transport fluid into their lumens after exposure to physiological levels of secretin or to inducers of cAMP [Talbot et al., 2002]. This was demonstrated in in vitro-derived bile ductules differentiated in culture from a pig liver cell line that originated from pig embryonic stem cells [Talbot et al., 2002]. AQP-1 and AQP-9 expression was detected by immunoblot in the cell line-derived ductules [Talbot et al., 2002], and the results presented here, therefore, illustrate that the in vitro-produced bile ductules are reproducing the expression pattern of AQP-1 and AQP-9 normally found in vivo, i.e. in the pig liver.

In conclusion, the study principally details the expression of AQP-1 and AQP-9 in fetal and adult pig liver tissue. AQP-1 cellular expression was found to be similar to that found in the rat. In contrast, AQP-9 liver expression was distinct from that found in the rat liver. This result suggests that AQP-9 may have a different functional role in the pig liver compared to the rat liver, and this is a similar finding to previous cross-species analyses where the expression patterns of AQPs were found to vary between human and rat [King and Agre, 2001].

Acknowledgments

We thank Dr. Lori Lana, Dr. Ransom Baldwin, Dr. Vernon G. Pursel and Dr. John M. Talbot for reading the manuscript and offering helpful editorial and scientific comments in its final preparation.

References

Agre, P., G.M. Preston, B.L. Smith, J.S. Jung, S. Raina, C. Moon, W.B. Guggino, S. Nielsen (1993) Aquaporin CHIP: The archetypical molecular water channel. Am J Physiol *265:* F463–F476.

Elkjær, J.L., Z. Vajda, L.N. Nejsum, T.H. Kwon, U.B. Jensen, M. Amiry-Moghaddam, J. Frøkiær, S. Nielsen (2000) Immunolocalization of AQP9 in liver, epididymis, testis, spleen and brain. Biochem Biophys Res Commun *276:* 1118–1128.

Engel A., Y. Fujiyoshi, P. Agre (2000) The importance of aquaporin water channel protein structures. EMBO J *19:* 800–806.

Enzan, H., H. Himeno, M. Hiroi, H. Kiyoku, T. Saibara, S. Onishi (1997) Development of hepatic sinusoidal structure with special reference to the Ito cells. Microsc Res Tech *39:* 336–349.

Frigeri, A., G.P. Nicchia, J.M. Verbavatz, G. Valenti, M. Svelto (1998) Expression of aquaporin-4 in fast-twitch fibers of mammalian skeletal muscle. J Clin Invest *102:* 695–703.

Gannon, B.J., G.M. Warnes, C.J. Carati, C.J. Verco (2000) Aquaporin-1 expression in visceral smooth muscle cells of the female rat reproductive tract. J Smooth Muscle Res *36:* 155–167.

Garcia, F., A. Kierbel, M.C. Larocca, S.A. Gradilone, P. Splinter, N.F. LaRusso, R.A. Marinelli (2001) The water channel aquaporin-8 is mainly intracellular in rat hepatocytes, and its plasma membrane insertion is stimulated by cyclic AMP. J Biol Chem *276:* 12147–12152.

Garrett, W.M., H.D. Guthrie (1996) Expression of androgen receptors and steroidogenic enzymes in relation to follicular growth and atresia following ovulation in pigs. Biol Reprod *55:* 949–955.

Huebert, R.C., P.L. Splinter, F. Garcia, R.A. Marinelli, N.F. LaRusso (2002) Expression and localization of aquaporin water channels in rat hepatocytes. J Biol Chem *277:* 22710–22717.

Ishibashi, K., K. Yamauchi, Y. Kageyama, F. Saito-Ohara, T. Ikeuchi, S. Ma (1998) Molecular characterization of human aquaporin-7 gene and its chromosomal mapping. Biochim Biophys Acta *1399:* 62–66.

King, L.S., P. Agre (2001) Man is not a rodent: Aquaporins in the airways. Am J Respir Cell Mol Biol *24:* 224–234.

Ma, T., A.S. Verkman (1999) Aquaporin water channels in gastrointestinal physiology. J Physiol *517:* 317–326.

Marinelli, R.A., N.F. LaRusso (1997) Aquaporin water channels in liver: Their significance in bile formation. Hepatology *26:* 1081–1084.

Marinelli, R.A., P.S. Tietz, L.D. Pham, L. Rueckert, P. Agre, N.F. LaRusso (1999) Secretin induces the apical insertion of aquaporin-1 water channels in rat cholangiocytes. Am J Physiol *276:* G280–G286.

Nerurkar, L.S., P.A. Marino, D.O. Adams (1981) Quantification of selected intracellular and secreted hydrolases of macrophages; in Herskowitz, H.B., H.T. Holden, J.A. Bellanti, A. Ghaffar (eds): Manual of Macrophage Methodology. New York, Marcel Dekker, pp 229–247.

Nicchia, G.P., A. Frigeri, B. Nico, D. Ribatti, M. Svelto (2001) Tissue distribution and membrane localization of aquaporin-9 water channel: Evidence for sex-linked differences in liver. J Histochem Cytochem *49:* 1547–1556.

Nielsen, S., B.L. Smith, E.I. Christensen, P. Agre (1993) Distribution of the aquaporin CHIP in secretory and resorptive epithelia and capillary endothelia. Proc Natl Acad Sci USA *90:* 7275–7279.

Nihei, K., Y. Koyama, T. Tani, E. Yaoita, K. Ohshiro, L.P. Adhikary, I. Kurosaki, Y. Shirai, K. Hatakeyama, T. Yamamoto (2001) Immunolocalization of aquaporin-9 in rat hepatocytes and Leydig cells. Arch Histol Cytol *64:* 81–88.

Roberts, S.K., M. Yano, Y. Ueno, L. Pham, G. Alpini, P. Agre, N.F. LaRusso (1994) Cholangiocytes express the aquaporin CHIP and transport water via a channel-mediated mechanism. Proc Natl Acad Sci USA *91:* 13009–13013.

Schrier, R.W., M.A. Cadnapaphornchai, M. Ohara (2001) Water retention and aquaporins in heart failure, liver disease and pregnancy. J Roy Soc Med *94:* 265–269.

Schulte, D.J., A.N. van Hoek (1997) Functional analysis and association state of water channel (AQP-1) isoforms purified from six mammals. Comp Biochem Physiol B Biochem Mol Biol *118:* 35–43.

Shi, L.B., W.R. Skach, A.S. Verkman (1994) Functional independence of monomeric CHIP28 water channels revealed by expression of wild type-mutant heterodimers. J Biol Chem *269:* 10417–10422.

Talbot, N.C., T.J. Caperna (1998) Selective and organotypic culture of intrahepatic bile duct cells from adult pig liver. In Vitro Cell Dev Biol *34A:* 785–798.

Talbot, N.C., T.J. Caperna, L.T. Lebow, D. Moscioni, V.G. Pursel, C.E. Rexroad, Jr. (1996) Ultrastructure, enzymatic, and transport properties of the PICM-19 bipotent liver cell line. Exp Cell Res *225:* 22–34.

Talbot, N.C., W. Garrett, T.J. Caperna (2002) The PICM-19 cell line as in vitro model of liver bile ductules: Effects of cAMP inducers, biopeptides and pH. Cells Tissues Organs *171:* 99–116.

Tani, T., Y. Koyama, K. Nihei, S. Hatakeyama, K. Ohshiro, Y. Yoshida, E. Yaoita, Y. Sakai, K. Hatakeyama, T. Yamamoto (2001) Immunolocalization of aquaporin-8 in rat digestive organs and testis. Arch Histol Cytol *64:* 159–168.

Timens, W., W.A. Kamps (1997) Hemopoiesis in human fetal and embryonic liver. Microsc Res Tech *39:* 387–397.